Artificial Intelligence in the Evaluation of Body Composition

Benjamin Wang, MD[1] Martin Torriani, MD, MMSc[1]

[1] Division of Musculoskeletal Imaging and Intervention, Department of Radiology, Massachusetts General Hospital, Harvard Medical School, Boston, Massachusetts

Address for correspondence Martin Torriani, MD, MMSc, Division of Musculoskeletal Imaging and Intervention, Department of Radiology, Massachusetts General Hospital, 55 Fruit Street, YAW 6048, Boston, MA 02114 (e-mail: mtorriani@mgh.harvard.edu).

Semin Musculoskelet Radiol 2020;24:30–37.

Abstract

Body composition entails the measurement of muscle and fat mass in the body and has been shown to impact clinical outcomes in various aspects of human health. As a result, the need is growing for reliable and efficient noninvasive tools to measure body composition. Traditional methods of estimating body composition, anthropomorphic measurements, dual-energy X-ray absorptiometry, and bioelectrical impedance, are limited in their application. Cross-sectional imaging remains the reference standard for body composition analysis and is accomplished through segmentation of computed tomography and magnetic resonance imaging studies. However, manual segmentation of images by an expert reader is labor intensive and time consuming, limiting its implementation in large-scale studies and in routine clinical practice. In this review, novel methods to automate the process of body composition measurement are discussed including the application of artificial intelligence and deep learning to tissue segmentation.

Keywords

- body composition analysis
- metabolic imaging
- artificial intelligence
- machine learning
- neural networks

Importance of Body Composition

Introduction

Body composition analysis refers to the quantitative and qualitative measurement and characterization of differing tissue types that make up the human body. Differences in body composition exist between men and women, and it has a critical influence in multiple health conditions.[1–3] As such, scientific interest in body composition is growing along with an increasing need for techniques to assess body composition accurately.

Adipose Tissue

Body composition studies have traditionally focused on the quantity of adipose tissue in the body. Adipose tissue is loose connective tissue composed of adipocytes that serve the primary function of energy storage in addition to providing cushion and insulation for the body. Growing evidence has demonstrated the critical role of adipose tissue in endocrinologic signaling and its role in various pathologic conditions. With the obesity epidemic, there is urgent need to better understand the physiologic impacts of adipose tissue and noninvasive methods for reliable quantification and characterization.

Women on average possess a higher body fat percentage compared with men of the same body mass index (BMI), but they tend to accumulate greater proportions of adipose tissue in the gluteal-femoral region. In contrast, men tend to accumulate adipose tissue in the abdominal region.[4] It has been well established that distribution of body fat has a greater impact on cardiometabolic risk than total body fat content, with abdominal fat conveying greater risk.

As such, abdominal adipose tissue has been extensively investigated in body composition studies. Adipose tissue is traditionally divided into two main compartments: subcutaneous adipose tissue (SAT) and visceral adipose tissue (VAT). VAT, the intra-abdominal adipose tissue that surrounds the visceral organs, has been linked to a variety of adverse health outcomes. Increased VAT was shown to be linked to metabolic derangements including impaired glucose and lipid metabolism,[2,3,5] contributing to cardiometabolic risk and all-cause

Issue Theme Musculoskeletal Applications of Artificial Intelligence; Guest Editors, Soterios Gyftopolous, MD, MSc and Naveen Subhas, MD, MPH

DOI https://doi.org/10.1055/s-0039-3400267.
ISSN 1089-7860.

mortality.[3,6,7] It was also shown to be associated with decreased bone mineral density,[8,9] nonalcoholic fatty liver disease,[10,11] and increased risk of malignancies.[12–14]

Muscle

More recently, body composition studies have increasingly emphasized the importance of muscle mass. Sarcopenia is a condition characterized by progressive and generalized loss of skeletal muscle mass and function that has important health implications.[15] Although consensus definitions have characterized sarcopenia as both diminished total muscle mass and decreased muscle function, reduced muscle mass on imaging studies remains an important focus of sarcopenia. There is increasing evidence in the literature linking sarcopenia to undesirable patient outcomes. For example, sarcopenia was associated with increased post–liver transplant mortality,[16] morbidity and mortality following colorectal surgery,[17] soft tissue sarcoma recurrence,[18] and increased mortality in hepatocellular carcinoma patients.[19] Sarcopenia was also linked to increased mortality and decreased ventilator-free days in intensive care unit patients.[20,21]

Miscellaneous

Although visceral adiposity and sarcopenia attract the greatest attention, other specialized body composition measurements have been examined including other ectopic foci of fat accumulation that are beyond the scope of this article. These include intermuscular adipose tissue (IMAT),[22] neck,[23] tongue,[24] and brown adipose tissue,[25] and the accumulation of lipids within skeletal muscle cells that affect insulin signaling and predispose to insulin resistance.[26]

Tools for Body Composition Measurements

Traditional Methods

Because of the clinical and prognostic implications of body composition, quick and reliable measurements are needed. Historically, many tools provided noninvasive estimates of body composition. These techniques include anthropomorphic measurements such as BMI, waist-to-hip ratio, and waist circumference. Although these measurements are inexpensive, quick, and easy to perform and may serve as noninvasive surrogates for fat mass, they are limited in accuracy. Other techniques that have been proposed include bioelectrical impedance analysis and dual-energy X-ray absorptiometry that have been validated as noninvasive techniques to estimate the total fat content in the body. However, these techniques are unable to distinguish between VAT and SAT and are therefore limited in providing detailed information on critical adipose compartments.[27]

Manual Image Segmentation

The accepted reference standard for body composition measurement involves segmentation of cross-sectional computed tomography (CT) and magnetic resonance imaging (MRI) by an expert reader.[28] However, manual segmentation of images is a time-consuming task. In our experience, a single axial CT slice at the level of L4 can take up to 25 minutes for accurate segmentation into five tissues (SAT, VAT, muscle, bone, and other tissues). Therefore, it is difficult to implement manual segmentation in large-scale epidemiologic studies and as part of clinical reporting. As a result, several tools have been developed to facilitate or automate the process of image segmentation.

Image Thresholding and Region Growing

The oldest and best established semiautomated method of image segmentation involves pixel thresholding, with or without the addition of region growing. In simple pixel thresholding, a lower and upper limit of pixel values are set by the user; all pixels in the image that fall within the preset range are then selected and are applicable to both CT and MRI studies. For segmentation of medical images, however, pixel thresholding alone has limited value. Furthermore, in the case of body composition measurements, pixel thresholding has no capability to distinguish VAT from SAT. As a result, pixel thresholding is usually combined with a region growing algorithm to improve segmentation performance by adding anatomical specificity and compartmentalizing segmented areas. Region growing is a category of image segmentation techniques that uses selected seed points to grow a region of pixels by iteratively examining neighboring pixels to determine if the pixels should be added to the region based on predefined criteria.[29]

Pixel thresholding with region growing is the primary approach for semiautomated image segmentation used in software packages such as Slice-o-matic (Tomovision, Montreal, Canada), National Institutes of Health (NIH) ImageJ (NIH, Bethesda, MD), Osirix (Pixmeo, Geneva, Switzerland), and Horos (Horos Project, Horosproject.org). These techniques are frequently used in the literature and remain the reference standard against which other techniques are benchmarked[30–32] (►**Fig. 1**). However, segmentations generated by these software packages require manual inspection and editing by an expert reader.

Fuzzy c-means Clustering

An alternative method to pixel thresholding for image segmentation involves the use of fuzzy c-means clustering (FCM), a method of unsupervised data classification that can identify different tissues in an image without the use of an explicit threshold value. Due to field homogeneities, pixel values in MR images do not fall within well-defined pixel ranges as they do in the case of CT images. As such, pixel thresholding techniques are less robust in segmenting MRI. FCM-based algorithms, combined with histogram thresholding, have provided robust segmentation of fat pixels on MRI images of the abdomen and thigh in an unsupervised and automated fashion when compared with manual techniques.[33–35] Briefly, the FCM algorithm implements fuzzy logic in an iterative fashion to assign membership of pixels to a specified number of classes. The fuzzy membership function, which takes a value of 0 to 1, reflects the level of similarity between the image pixel of interest and the prototypical data or centroid of its class.[33,34]

In the context of body composition analysis, FCM algorithms have been used to coarsely segment a MR image into

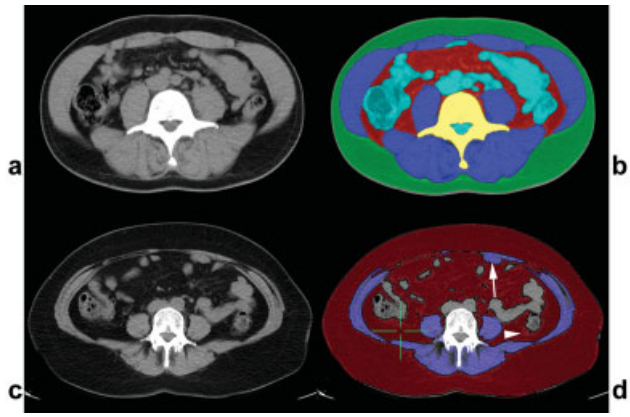

Fig. 1 (**a**) Noncontrast computed tomography axial images obtained at the level of L4. (**b**) Typical manual segmentation of tissue compartments for body composition analysis using thresholding and region growing: subcutaneous (green) and visceral (red) adipose tissue, muscle (blue), bone (yellow), and other tissues (cyan). Performed manually by an expert operator, this single-image segmentation can take up to 25 minutes to accomplish. (**c, d**) Segmentation of visceral adipose tissue (VAT) (red) and muscle (blue) on a different patient using thresholding and region growing before manual editing by a radiologist. Seed point for segmentation of VAT is placed in the adipose tissue surrounding the right colon (green crosshair). Note that the region growing algorithm is unable to distinguish VAT from subcutaneous adipose tissue and that parts of the bowel are incorrectly labeled as VAT (white arrowhead). Also note that the region growing algorithm incorrectly labels a loop of bowel as muscle (white arrow). These errors all require manual editing by an expert reader.

fat tissue, nonfat tissue, and background (►**Fig. 2**). These FCM algorithms are then generally combined with a method of anatomical localization to distinguish VAT from SAT.[36] The most common method to achieve this is through the detection of the muscle layer between subcutaneous and visceral fat through the use of curve deformation methods, often referred to as "snakes."[33,34,37] After the muscle boundaries are determined, histogram thresholding is then used to calculate the total pixels of VAT within the bounds of the abdominal wall.[35]

Multi-atlas Segmentation

Multi-atlas segmentation is a more recent method of image segmentation that has been developed and implemented for the purpose of body composition analysis. In brief, atlas-guided segmentation algorithms are a form of supervised learning algorithms that use manually pre-segmented atlases to assign segmentation labels to an image. In such an algorithm, an image is spatially registered to the prelabeled atlas through a series of computationally expensive deformation steps until the two images are similar. The resulting mapping between the coordinates of the two images is then used to propagate the segmentation labels from the atlas to the new image.[38]

However, due to the anatomical variation that exists between individuals and slight differences in patient positioning during imaging, there are substantial limitations to accurate mapping of an image if only a single atlas image was available. As such, a more elegant approach using a library of atlases has been developed to capture the variation that exists and is referred to as multi-atlas segmentation (MAS). In MAS, the novel image is registered with each atlas within the library in a pairwise fashion, and the results are used to label the image through a "majority voting" system where the most frequently chosen label is used.

MAS techniques have been proven effective in the field of body composition analysis. Examples in the literature include MAS-based techniques to segment muscle, VAT, and SAT on full-body three-dimensional data sets from attenuation correction CTs of positron emission tomography/computed tomography examinations[39] as well as techniques to segment VAT and SAT on full-body MRI.[40] Additional implementations of MAS also include multiorgan segmentation on abdominal CTs and muscle segmentation on whole-body MRI[41] (►**Fig. 3**).

MAS techniques are robust and have a distinct advantage of requiring a relatively small amount of a priori data to

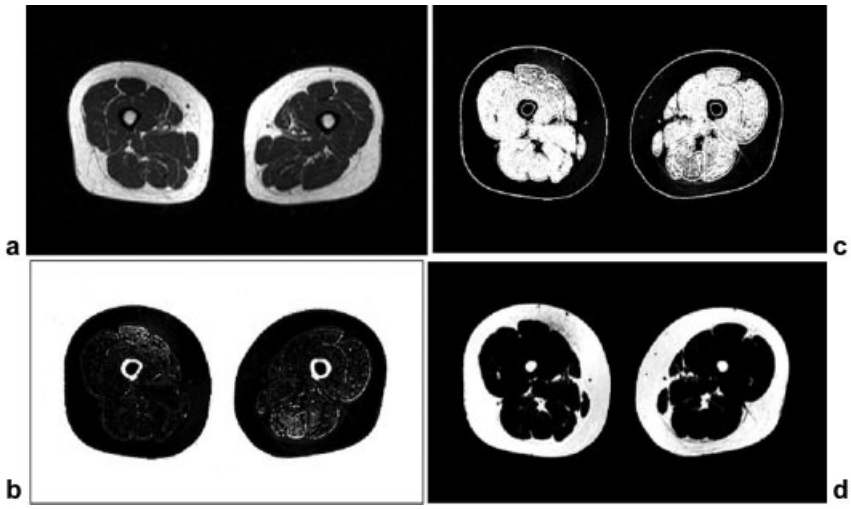

Fig. 2 (**a**) T1-weighted axial image of bilateral thighs with membership maps from fuzzy clustering segmentation. (**b**) Background and bone, (**c**) muscle, and (**d**) fat maps are shown, with brighter pixels indicating higher membership values. Subsequent processing steps using "snakes" (not shown) to identify boundaries of muscle and bone are required to separate subcutaneous adipose tissue from intermuscular adipose tissue. Mean processing time per slice was 52 ± 7 seconds (Intel PC, 3.2 GHz, 2 GB RAM, Windows 2000 OS). (Reprinted with permission from Positano et al.[33])

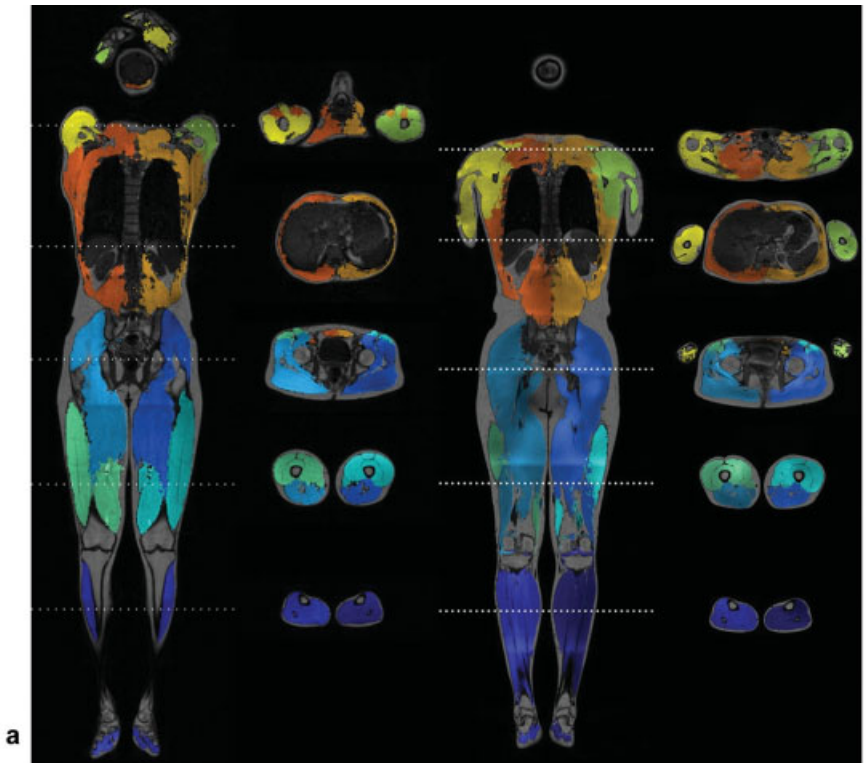

Fig. 3 Example of atlas with 10 muscle labels overlaid on magnetic resonance image at (**a**) 1.5 T and (**b**) 3.0 T. The several labels used in the atlas allow for differentiation of specific muscles and patient side. Average processing time per case was not reported. (Reprinted with permission from Karlsson et al.[41])

achieve acceptable segmentation performance. However, its major limitation is the high computational resources required at the time of deployment to segment each novel case.[38] Each new case presented to the tool requires the system to perform numerous registration tasks with a full library of atlases, a process that is computationally demanding and requires a substantial amount of time. Decazes et al reports that their MAS-based tool for segmentation of muscle, VAT, and SAT on attenuation correction CTs required $\sim$ 25 minutes to segment each case.[39] Although computational speed will undoubtedly increase as technology advances, this could be offset by increasing the complexity of algorithms.

Artificial Intelligence and Deep Learning

Overview

Artificial intelligence (AI) and deep machine learning (ML) have recently garnered increased attention in the scientific community and mainstream media. Although the terms "artificial intelligence" and "machine learning" are often used interchangeably, they are not synonymous. AI can be understood as a system or machine that can mimic human cognition to accomplish certain tasks. It can also be thought of as any system that can use data to help guide or influence its actions. ML, in contrast, refers more specifically to a system or algorithm that is capable of learning and improving through the use of data. As such, ML is a method through which AI can be achieved.

Recent advancements in hardware capabilities and algorithm development have led to the increased popularity of ML. Although ML can be applied to a wide spectrum of clinical tasks and workflow in radiology, applications focused on automating repetitive and tedious tasks will likely have the greatest impact. Tasks such as image segmentation and quantitative image analysis are particularly well suited for ML algorithms because human readers tend to be inefficient or inaccurate at performing these tasks. Focusing ML development in these areas can help improve radiologist performance by augmenting radiologists in areas where they are naturally ineffective, allowing them to focus effort in areas of strength (e.g., high-level diagnosis and synthesis of clinical data).

Neural Networks

Currently, a popular framework for ML in imaging is the artificial neural network. An artificial neural network can be thought of as a digital model that simulates the cellular framework of the brain. These models consist of numerous interconnected nodes, with each node emulating the behavior of a neuron and the connections acting as synapses between neurons.

Neural networks are generally organized in layers of nodes, with each additional layer and node adding to the complexity and versatility of the model. With sufficient depth, a neural network is capable of simulating complex relationships between data. In a traditional neural network, all nodes in the network share a connection with every node

in the preceding and subsequent layer and are therefore considered "fully connected."

Convolutional Neural Network

A variant of the neural network, the convolutional neural network (CNN), was shown to be particularly effective at visual recognition and computer vision tasks, particularly with the task of semantic image classification. In 2012, Krizhevsky et al introduced a CNN at the annual ImageNet competition (ImageNet Large-Scale Visual Recognition Challenge) and beat the nearest competitor by a 41% margin in an image classification task.[42] In the years to follow, more complex CNNs would be introduced and achieve classification error rates that were lower than human benchmarks for a similar task.[43,44]

CNNs take advantage of the spatial relationship of pixels in imaging data to greatly reduce the complexity and required parameters of a neural network. CNNs replace the fully connected architecture of traditional neural networks with a computationally less demanding series of convolution and data pooling operations. A convolution operation takes a set of image filters with a limited receptive field (e.g., 3×3 or 5×5 pixels), marches it across the image at a predetermined stride length, and computes the dot product between the image pixels and the filter at each step. Doing so generates two-dimensional activation maps for each filter that are then sent to the next layer of the network. Convolution is typically followed by a data pooling operation that reduces the dimensions of the data by combining the output of the previous layer in clusters (typically 2×2), effectively cutting the dimensions of the data in half. A series of these convolution and pooling operations results in a progressively contracting network architecture that takes high-resolution pixel-level information and aggregates it into high-level semantic information. The final layers of the CNN typically consist of a few fully connected layers before generating an output[42] (►**Fig. 4**).

Fully Convolutional Neural Networks

Traditional CNN architectures such as AlexNet and ResNet demonstrated high accuracy at image classification tasks and were implemented successfully in a limited capacity in clinical imaging tasks.[45,46] As CNNs have gained popularity, adaptations of CNN architectures have been developed to allow for pixel-level semantic segmentation of images. Known as fully CNNs, these architectures are capable of not only determining what is contained within an image, but also to localize pixels of interest. A popular implementation of the fully convolutional neural network, the U-Net, achieves this by replacing the fully connected portion of the CNN with an additional series of convolution operations that are chained with up-sampling deconvolution operations. These up-sampling operations serve to serially increase the resolution of the output. In addition, at each up-sampling step, high-resolution features from the corresponding contracting path of the neural network are combined with the up-sampled output to improve spatial localization of sematic information. This architecture results in a generally symmetrical contracting and expansive path resulting in a U-shaped structure[47,48] (►**Fig. 5**).

Applications of Deep Learning in Body Composition Analysis

Deep Learning Algorithms for Image Segmentation

The availability of neural network architectures that allow for pixel-level image segmentation presents an opportunity for creating body composition analysis tools. Neural networks can be trained end to end, meaning the only data required for training are input data (a set of images) and corresponding output (a set of prelabeled segmentation maps). As a result, the development of a model based on a neural network is straightforward if training data are available. Furthermore, although the computational demands of training neural networks can be quite high, using a pretrained neural network to make predictions on novel data requires relatively minimal amounts of computing power, such that nearly any modern personal computer would be capable of running the model. This is in contrast to multiple atlas-based algorithms where significant computational demand occurs at the time of prediction.

The U-Net architecture has proven to be effective at segmentation of two-dimensional biomedical images. In the case of body composition analysis, Bridge et al demonstrated a U-Net is

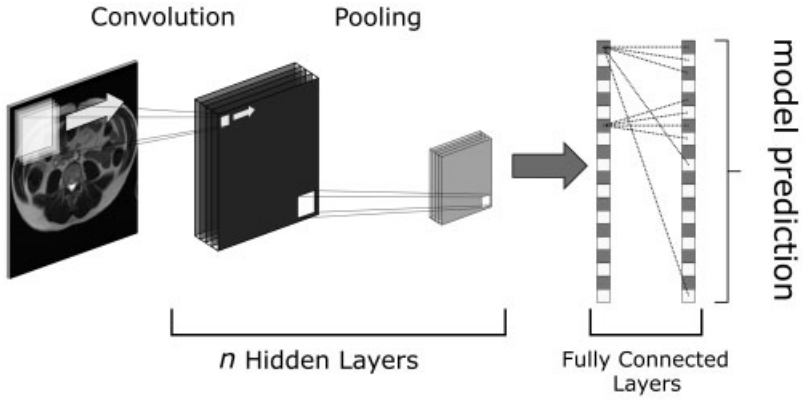

Fig. 4 Diagram illustrating the architecture of a convolutional neural network (CNN) showing a single convolution and pooling operation followed by a single fully connected layer (typical CNN architectures contain numerous consecutive convolution and pooling steps followed by several fully connected layers before prediction).

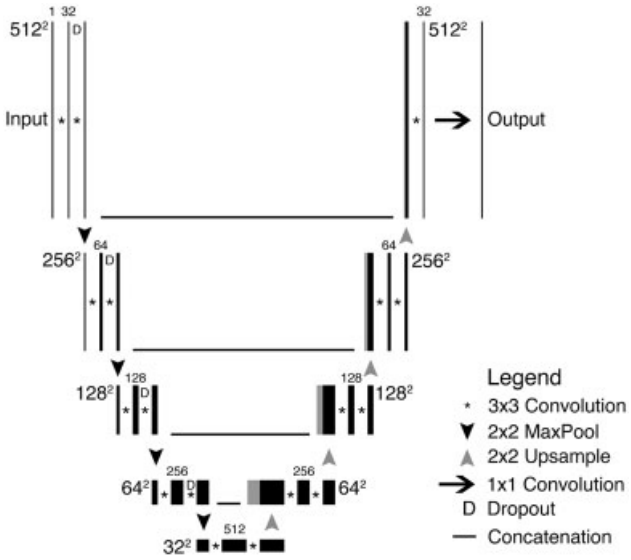

Fig. 5 Schematic illustrating the U-Net architecture. From left to right, the model architecture receives a 512 × 512-pixel grayscale image that goes through a series of convolution and pooling operations, sequentially reducing the dimensions of the data. This is followed by a series of up-sampling and convolution operations that increase the dimensions of the data back to the original 512 × 512 size. Additionally, at each up-sampling stage, data from the equivalent contracting limb are concatenated with the data matrix to help improve spatial localization of high-level semantic information to improve segmentation performance. The architecture results in a U-shaped network as illustrated. (Reprinted from Hemke et al.[53])

capable of segmenting VAT, SAT, and skeletal muscle on a single CT slice obtained at the L3 level with a high level of accuracy, achieving mean Dice scores of 0.95, 0.98, and 0.97 for VAT, SAT, and skeletal muscle, respectively.[49] This was accomplished with a data set of 595 manually segmented CT images divided into 412 training, 94 validation, and 89 test cases. Their trained model required 0.02 to 0.025 seconds to perform segmentations on novel cases while running on a Nvidia V100 GPU and 0.60 seconds while running on a central processing unit (CPU). These results prove that neural networks can create tools for body composition measurements that could be deployed in large-scale cohort studies. Furthermore, the speed at which such segmentations can be performed points toward easier adoption in a variety of clinical and research workflows (►**Fig. 6**).

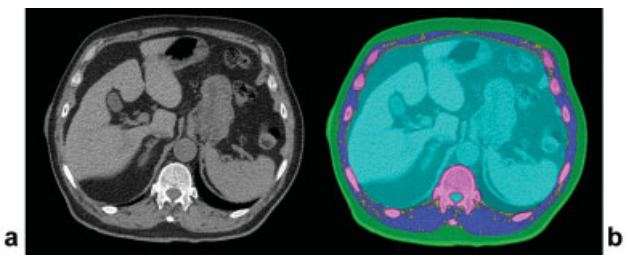

Fig. 6 (**a**) Noncontrast computed tomography axial image obtained at the level of T12. (**b**) Automated segmentation of tissue compartments for body composition analysis using U-Net CNN: subcutaneous (green) and intermuscular (yellow) adipose tissue, muscle (blue), bone (magenta), and other tissues (cyan). This segmentation was generated on a CPU in 4.3 seconds.

Weston et al expanded on the previously published work by training a U-Net to segment a total of five tissue classes (muscle, bone, visceral fat-free tissue, SAT, and VAT) on a single CT slice at L3 using a data set of 2,700 studies (2,430 for training and 270 for test data set). Dice scores for each tissue class were 0.96 (muscle), 0.98 (bone), 0.97 (visceral fat-free tissue), 0.98 (SAT), and 0.94 (VAT). In addition, Weston and colleagues demonstrated the generalizability of the trained model to perform image segmentation at a different anatomical level. In their study, they demonstrate no statistically significant difference in model performance for identifying the SAT, muscle, and visceral compartment when implemented on novel CT images acquired at L3 and L4 (model trained only on images acquired at L3).[50]

Accelerating the Development of Deep Learning Algorithms

The work of Bridge et al and Weston et al demonstrates promise in implementing deep learning algorithms for body composition measurements. However, the large amount of training data needed to effectively train deep learning algorithms limits the speed at which algorithms can be developed and deployed. Additionally, because deep learning algorithm performance is highly specific to the data set on which the model was trained, it may be difficult to generalize a model trained at one institution to another where imaging parameters and protocols are different. One solution to this problem would be to build a training data set containing labeled images from numerous institutions with differing imaging protocols and parameters. However, doing so further increases the burden of creating a sufficiently large data set.

Alternatively, further work has been pursued, building on the work by Bridge et al and Weston et al, by implementing data augmentation to train a U-Net with a relatively small number of training examples. Data augmentation is a resource in ML that allows for greatly expanding a limited training data set through random image transformations such as deformations, horizontal mirroring, cropping, magnification, and addition of noise. Doing so facilitates training neural networks with small data sets, such as those commonly encountered in biomedical research studies.[48,51] In our experience, preliminary results demonstrate that a U-Net trained with a limited number of training examples ($n = 140$) yielded an overall mean Dice score of 96%, with individual tissue class Dice scores of 87% (bone), 91% (muscle), 89% (bowel/solid organs), 94% (SAT), and 81% (VAT).[52] A similar workflow can be applied to body composition measurements in other anatomical areas, such as assessment of muscle mass in the pelvis. Using a similar technique, we trained a U-Net model with a training data set of 200 CT images of the pelvis at the level of the acetabular roof. With data augmentation, the model was trained to segment the pelvic cavity, SAT, muscle, IMAT, and bone, yielding Dice scores of 0.98, 0.97, 0.95, 0.91, and 0.92, respectively.[53] These results demonstrate the feasibility of using data augmentation to rapidly prototype neural network models to perform body composition measurements at varying anatomical locations (►**Fig. 7**).

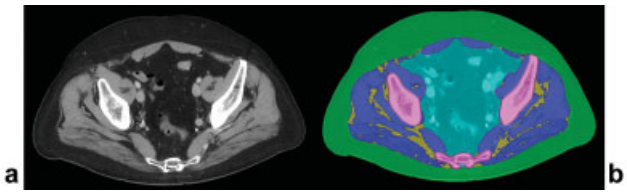

Fig. 7 (**a**) Post intravenous contrast computed tomography axial image obtained at the level of the acetabular roof for measurement of body composition at the pelvis. (**b**) Automated segmentation of tissue compartments using U-Net convolutional neural network: subcutaneous (green) and intermuscular (yellow) adipose tissue, muscle (blue), bone (magenta), and other tissues (cyan). This segmentation was generated on a CPU in 4.1 seconds.

Deep Learning Body Composition Tools in Practice

With several deep learning models for body composition measurements in hand, future development will involve integration of trained models into clinical and/or scientific workflows. This represents a critical step because it will allow delivery of valuable metabolic information in tandem with traditional imaging reports. An example of this workflow would be information such as muscle mass, VAT, and SAT content being automatically measured in the background from abdominal CTs obtained for various indications (cancer, staging, etc.) and inserted into reporting systems. This type of workflow can be highly desirable because the cost of image acquisition is obviated by the original indication; however, prognostic body composition information can be obtained with high accuracy, adding value to the patient's care. With the increasing body of evidence linking various body composition measurements to patient outcomes, having this data readily available to clinicians and scientists will greatly accelerate the development of improved predictive models and treatment algorithms.

Conclusion

Body composition has a significant impact on health outcomes in a wide variety of clinical settings. As such, the need for reliable and fast methods to measure body composition continues to grow. Traditional standards to perform these measurements through manual segmentation of cross-sectional imaging studies is labor intensive and time consuming, severely limiting widespread adoption. Innovations in ML and neural networks have provided novel applications to automate body composition analysis. CNNs can quickly and accurately segment cross-sectional images and be deployed without need for advanced hardware. As a result, trained neural networks can more readily be implemented for large-scale studies and widespread clinical use. Furthermore, given the characteristics of this technology, it is more feasible to develop algorithms that can manage volumetric data (i.e., full image stacks from a CT or MRI). In summary, technological advance introduced by AI and ML have contributed to make body composition data more easily available, allowing health care professionals to better care for patients and advance scientific research in large cohorts.

Funding Source
Martin Torriani was funded in part by the National Institutes of Health Nutrition and Obesity Research Center at Harvard University (P30 DK040561).

Conflict of Interest
None declared.

References

1 Bredella MA. Sex differences in body composition. Adv Exp Med Biol 2017;1043:9–27
2 Ritchie SA, Connell JMC. The link between abdominal obesity, metabolic syndrome and cardiovascular disease. Nutr Metab Cardiovasc Dis 2007;17(04):319–326
3 Fox CS, Massaro JM, Hoffmann U, et al. Abdominal visceral and subcutaneous adipose tissue compartments: association with metabolic risk factors in the Framingham Heart Study. Circulation 2007;116(01):39–48
4 Lemieux S, Prud'homme D, Bouchard C, Tremblay A, Després JP. Sex differences in the relation of visceral adipose tissue accumulation to total body fatness. Am J Clin Nutr 1993;58(04):463–467
5 Björntorp P. Metabolic abnormalities in visceral obesity. Ann Med 1992;24(01):3–5
6 Rosenquist KJ, Pedley A, Massaro JM, et al. Visceral and subcutaneous fat quality and cardiometabolic risk. JACC Cardiovasc Imaging 2013;6(07):762–771
7 Rosenquist KJ, Massaro JM, Pedley A, et al. Fat quality and incident cardiovascular disease, all-cause mortality, and cancer mortality. J Clin Endocrinol Metab 2015;100(01):227–234
8 Schorr M, Dichtel LE, Gerweck AV, Torriani M, Miller KK, Bredella MA. Body composition predictors of skeletal integrity in obesity. Skeletal Radiol 2016;45(06):813–819
9 Bredella MA, Torriani M, Ghomi RH, et al. Determinants of bone mineral density in obese premenopausal women. Bone 2011;48 (04):748–754
10 Eguchi Y, Eguchi T, Mizuta T, et al. Visceral fat accumulation and insulin resistance are important factors in nonalcoholic fatty liver disease. J Gastroenterol 2006;41(05):462–469
11 van der Poorten D, Milner KL, Hui J, et al. Visceral fat: a key mediator of steatohepatitis in metabolic liver disease. Hepatology 2008;48(02):449–457
12 Oh TH, Byeon JS, Myung SJ, et al. Visceral obesity as a risk factor for colorectal neoplasm. J Gastroenterol Hepatol 2008;23(03): 411–417
13 Schapira DV, Clark RA, Wolff PA, Jarrett AR, Kumar NB, Aziz NM. Visceral obesity and breast cancer risk. Cancer 1994;74(02): 632–639
14 von Hafe P, Pina F, Pérez A, Tavares M, Barros H. Visceral fat accumulation as a risk factor for prostate cancer. Obes Res 2004; 12(12):1930–1935
15 Santilli V, Bernetti A, Mangone M, Paoloni M. Clinical definition of sarcopenia. Clin Cases Miner Bone Metab 2014;11(03):177–180
16 Englesbe MJ, Patel SP, He K, et al. Sarcopenia and mortality after liver transplantation. J Am Coll Surg 2010;211(02):271–278
17 Reisinger KW, van Vugt JLA, Tegels JJW, et al. Functional compromise reflected by sarcopenia, frailty, and nutritional depletion predicts adverse postoperative outcome after colorectal cancer surgery. Ann Surg 2015;261(02):345–352
18 De Amorim Bernstein K, Bos SA, Veld J, Lozano-Calderon SA, Torriani M, Bredella MA. Body composition predictors of therapy response in patients with primary extremity soft tissue sarcomas. Acta Radiol 2018;59(04):478–484
19 Fujiwara N, Nakagawa H, Kudo Y, et al. Sarcopenia, intramuscular fat deposition, and visceral adiposity independently predict the outcomes of hepatocellular carcinoma. J Hepatol 2015;63(01): 131–140

20 Moisey LL, Mourtzakis M, Cotton BA, et al; Nutrition and Rehabilitation Investigators Consortium (NUTRIC). Skeletal muscle predicts ventilator-free days, ICU-free days, and mortality in elderly ICU patients. Crit Care 2013;17(05):R206

21 Weijs PJM, Looijaard WGPM, Dekker IM, et al. Low skeletal muscle area is a risk factor for mortality in mechanically ventilated critically ill patients. Crit Care 2014;18(02):R12

22 Gallagher D, Kuznia P, Heshka S, et al. Adipose tissue in muscle: a novel depot similar in size to visceral adipose tissue. Am J Clin Nutr 2005;81(04):903–910

23 Torriani M, Gill CM, Daley S, Oliveira AL, Azevedo DC, Bredella MA. Compartmental neck fat accumulation and its relation to cardiovascular risk and metabolic syndrome. Am J Clin Nutr 2014;100 (05):1244–1251

24 Godoy IRB, Martinez-Salazar EL, Eajazi A, Genta PR, Bredella MA, Torriani M. Fat accumulation in the tongue is associated with male gender, abnormal upper airway patency and whole-body adiposity. Metabolism 2016;65(11):1657–1663

25 Sampath SC, Sampath SC, Bredella MA, Cypess AM, Torriani M. Imaging of brown adipose tissue: state of the art. Radiology 2016; 280(01):4–19

26 Torriani M, Thomas BJ, Barlow RB, Librizzi J, Dolan S, Grinspoon S. Increased intramyocellular lipid accumulation in HIV-infected women with fat redistribution. J Appl Physiol (1985) 2006;100 (02):609–614

27 Shuster A, Patlas M, Pinthus JH, Mourtzakis M. The clinical importance of visceral adiposity: a critical review of methods for visceral adipose tissue analysis. Br J Radiol 2012;85(1009):1–10

28 Maurovich-Horvat P, Massaro J, Fox CS, Moselewski F, O'Donnell CJ, Hoffmann U. Comparison of anthropometric, area- and volume-based assessment of abdominal subcutaneous and visceral adipose tissue volumes using multi-detector computed tomography. Int J Obes 2007;31(03):500–506

29 Pal NR, Pal SK. A review on image segmentation techniques. Pattern Recognit 1993;26(09):1277–1294

30 Ross R, Léger L, Guardo R, De Guise J, Pike BG. Adipose tissue volume measured by magnetic resonance imaging and computerized tomography in rats. J Appl Physiol (1985) 1991;70(05): 2164–2172

31 Ross R, Léger L, Morris D, de Guise J, Guardo R. Quantification of adipose tissue by MRI: relationship with anthropometric variables. J Appl Physiol (1985) 1992;72(02):787–795

32 Irving BA, Weltman JY, Brock DW, Davis CK, Gaesser GA, Weltman A. NIH ImageJ and Slice-O-Matic computed tomography imaging software to quantify soft tissue. Obesity (Silver Spring) 2007;15 (02):370–376

33 Positano V, Christiansen T, Santarelli MF, Ringgaard S, Landini L, Gastaldelli A. Accurate segmentation of subcutaneous and intermuscular adipose tissue from MR images of the thigh. J Magn Reson Imaging 2009;29(03):677–684

34 Positano V, Gastaldelli A, Sironi AM, Santarelli MF, Lombardi M, Landini L. An accurate and robust method for unsupervised assessment of abdominal fat by MRI. J Magn Reson Imaging 2004;20(04):684–689

35 Lancaster JL, Ghiatas AA, Alyassin A, Kilcoyne RF, Bonora E, DeFronzo RA. Measurement of abdominal fat with T1-weighted MR images. J Magn Reson Imaging 1991;1(03):363–369

36 Tang Y, Sharma P, Nelson MD, Simerly R, Moats RA. Automatic abdominal fat assessment in obese mice using a segmental shape model. J Magn Reson Imaging 2011;34(04):866–873

37 Kass M, Witkin A, Terzopoulos D. Snakes: active contour models. Int J Computer Vision 1988;1:321–331

38 Iglesias JE, Sabuncu MR. Multi-atlas segmentation of biomedical images: a survey. Med Image Anal 2015;24(01):205–219

39 Decazes P, Tonnelet D, Vera P, Gardin I. Anthropometer3D: Automatic multi-slice segmentation software for the measurement of anthropometric parameters from CT of PET/CT. J Digit Imaging 2019;32(02):241–250

40 Kullberg J, Johansson L, Ahlström H, et al. Automated assessment of whole-body adipose tissue depots from continuously moving bed MRI: a feasibility study. J Magn Reson Imaging 2009;30(01): 185–193

41 Karlsson A, Rosander J, Romu T, et al. Automatic and quantitative assessment of regional muscle volume by multi-atlas segmentation using whole-body water-fat MRI. J Magn Reson Imaging 2015;41(06):1558–1569

42 Krizhevsky A, Sutskever I, Hinton GE. ImageNet classification with deep convolutional neural networks. In: Pereira F, Burges CJC, Bottou L, Weinberger KQ, eds. Advances in Neural Information Processing Systems 25. Red Hook, NY: Curran Associates; 2012: 1097–1105

43 He K, Zhang X, Ren S, Sun J. Deep residual learning for image recognition. In: Proceedings of 2016 IEEE Conference on Computer Vision and Pattern Recognition (CVPR). Vol 46. New York, NY: IEEE; 2016:770–778

44 He K, Zhang X, Ren S, Sun J. Delving deep into rectifiers: surpassing human-level performance on ImageNet classification. In: Proceedings of 2015 IEEE International Conference on Computer Vision (ICCV). Vol 86. New York, NY: IEEE; 2015:1026–1034

45 Lehman CD, Yala A, Schuster T, et al. Mammographic breast density assessment using deep learning: clinical implementation. Radiology 2019;290(01):52–58

46 Lee H, Tajmir S, Lee J, et al. Fully automated deep learning system for bone age assessment. J Digit Imaging 2017;30(04):427–441

47 Long J, Shelhamer E, Darrell T. Fully convolutional networks for semantic segmentation. In: Proceedings of 2015 IEEE Conference on Computer Vision and Pattern Recognition (CVPR). Vol 39. New York, NY: IEEE; 2015:3431–3440

48 Ronneberger O, Fischer P, Brox T. U-Net: convolutional networks for biomedical image segmentation. Med Image Comput Comput Interv 2015;9351:234–241

49 Bridge CP, Rosenthal M, Wright B, et al. Fully-automated analysis of body composition from CT in cancer patients using convolutional neural networks. In: Lecture Notes in Computer Science (Including Subseries Lecture Notes in Artificial Intelligence and Lecture Notes in Bioinformatics). Vol 11041. New York, NY: Springer; 2018:204–213

50 Weston AD, Korfiatis P, Kline TL, et al. Automated abdominal segmentation of CT scans for body composition analysis using deep learning. Radiology 2019;290(03):669–679

51 Perez L, Wang J. The effectiveness of data augmentation in image classification using deep learning. Clin Orthop Relat Res 2017. Abstract available at: https://arxiv.org/abs/1712.04621

52 Wang B, Buckless C, Tsao A, Torriani M. Multi-tissue segmentation for body composition using a deep convolutional neural network. Paper presented at: 104th Scientific Assembly and Annual Meeting of the RSNA; November 25–29, 2018; Chicago, IL

53 Hemke R, Buckless C, Tsao A, Wang B, Torriani M. Deep learning for automated segmentation of pelvic muscle mass from CT studies. Skelet Radiol 2019. Doi: 10.1007/s00256-019-03289-8